PHYSICAL REVIEW B **66**, 140408(R) (2002)

Change in charge and orbital alignment upon antiferromagnetic transition in the *A*-site-ordered perovskite manganese oxide $R\mathrm{BaMn_2O_6}$ (R=Tb and Sm)

T. Arima,[1,2] D. Akahoshi,[3] K. Oikawa,[4] T. Kamiyama,[4] M. Uchida,[5] Y. Matsui,[5] and Y. Tokura[1,3,6]

[1]*Spin Superstructure Project, ERATO, Japan Science and Technology (JST), Tsukuba 305-8562, Japan*

[2]*Institute of Materials Science, University of Tsukuba, Tsukuba 305-8573, Japan*

[3]*Correlated Electron Research Center (CERC), National Institute of Advanced Industrial Science and Technology (AIST), Tsukuba 305-8562, Japan*

[4]*Neutron Science Laboratory, Institute of Materials Structure Science, High Energy Accelerator Research Organization, Tsukuba 305-0801, Japan*

[5]*Advanced Materials Laboratory, National Institute for Materials Science (NIMS), Tsukuba 305-0044, Japan*

[6]*Department of Applied Physics, University of Tokyo, Tokyo 113-8656, Japan*

(Received 12 August 2002; published 30 October 2002)

A neutron-diffraction study on an *A-site-ordered* perovskite manganite $R\mathrm{BaMn_2O_6}$ (R=Tb) has revealed that the magnetic structure is characterized by two modulation vectors, (1/2 0 1/4) and (1/4 1/4 1/4), in the primitive cubic setting. The appearance of the magnetic order is accompanied by change in stacking of charge-ordered/orbital-ordered MnO_2 sheets along the c axis, which has also been confirmed by electron-diffraction and x-ray-diffraction studies on the R=Tb and Sm compounds. The charge ordering in the antiferromagnetic phase is an unprecedented one, i.e., NaCl type, which is stabilized by the ordering of R and Ba in the A site.

DOI: 10.1103/PhysRevB.66.140408 PACS number(s): 75.25.+z, 61.12.−q, 61.14.−x

After the discovery of colossal magnetoresistance (CMR) effect, the perovskite-related manganese oxide system has been extensively investigated. Among them, the close interplay between charge, orbital, and spin degrees of freedom is one of the key ingredients in the CMR science.[1] The ordering and disordering of each degree of freedom has been investigated as a function of many material parameters, such as the doping level, the average ionic radius of the A site, the difference of the A-site ionic radii, the number of the successive MnO_2 sheets, and so on. Recently, it has been reported that ordering of a rare-earth element R and barium in the A-site of perovskite structure significantly affects the electronic phase diagram of the manganese oxide compound.[2–4] The A-site ordering in $R_{1/2}\mathrm{Ba}_{1/2}\mathrm{MnO_3}$ (see the inset of Fig. 1) or $R\mathrm{BaMn_2O_6}$, with R=Sm, Eu, Gd, Tb, Dy, Ho, and Y seems to assist ordering of charge and orbital at a relatively high temperature, contrary to the case of the A-site-disordered compound with the same composition, which shows spin-glass behavior at low temperatures ($<$50 K).[4] It has been suggested that the spin-glass state could be due to the quenched potential disorder arising from large difference of the ionic radius between R and Ba and the resultant local lattice distortion. The A-site ordering reduces the effect of this disorder. Moreover, the ordering pattern of charge and orbital in the A-site-ordered manganites is recently found to be modified from the well-known charge/orbital ordering observed in the disordered compounds, $(R,\mathrm{Ca})\mathrm{MnO_3}$ and $(R,\mathrm{Sr})\mathrm{MnO_3}$.[1,5] While charge and orbital stripes align on the a-b plane in the same manner, the stacking along the c axis is accompanied by a regular phase shift in the A-site-ordered compound [see Fig. 2(a)].[6]

The magnetic structure of the charge-ordered/orbital-ordered manganese oxide with a Mn average valence of around 3.5+ is usually of the zigzag type in the a-b plane and antiferromagnetically arranged along the c axis [so-called charge exchange (CE)-type].[7,8] Since the magnetic structure is totally regulated by the charge/orbital ordering,[5] the A-site-ordered manganese oxide is likely to show a dif-

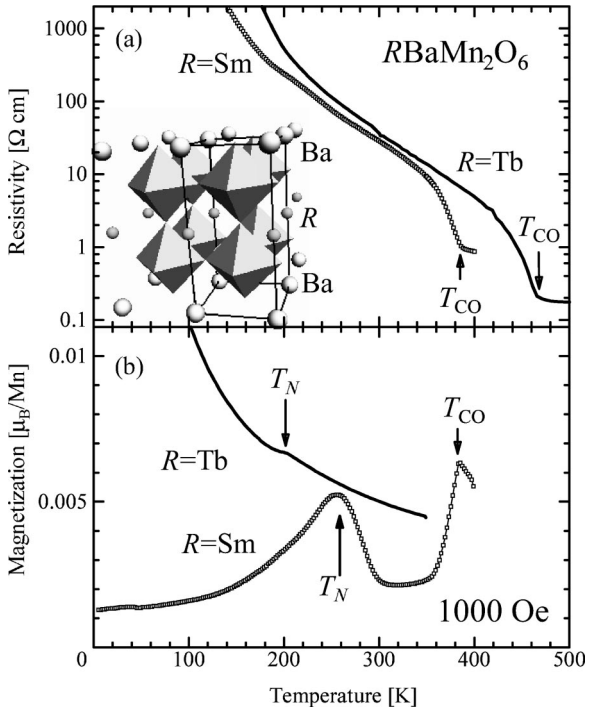

FIG. 1. (a) Resistivity and (b) magnetization of A-site-ordered $\mathrm{SmBaMn_2O_6}$ and $\mathrm{TbBaMn_2O_6}$, measured in warming runs. The measurement of magnetization was performed in a magnetic field of 0.1 T after zero-field cooling. Inset shows the schematic crystal structure of $R\mathrm{BaMn_2O_6}$. The attached box drawn with thin lines shows the primitive unit cell of $a_p \times a_p \times 2a_p$.

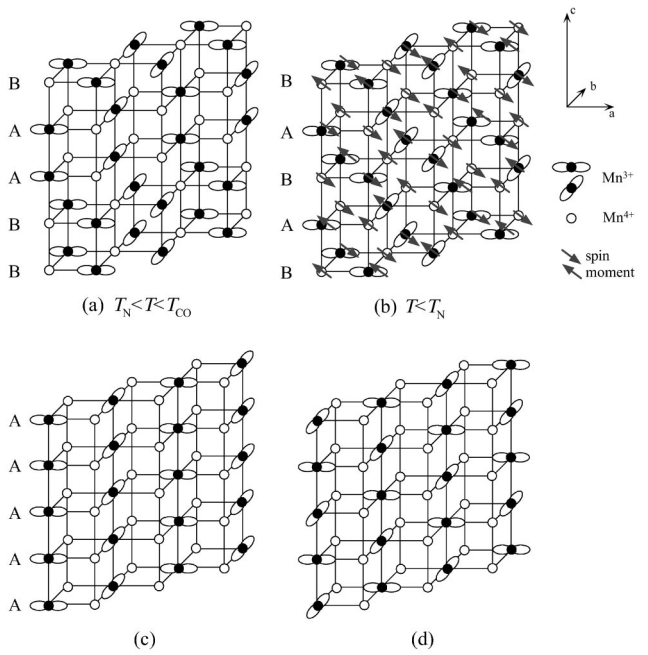

FIG. 2. Schematic drawing of the ordering pattern of charge, orbital, and spin in the *A*-site-ordered perovskite manganites $R\mathrm{BaMn_2O_6}$ ($R=$ Sm and Tb) for (a) $T_N<T<T_{\mathrm{CO}}$ and (b) $T<T_N$. (c) and (d) show other possibilities discussed in the text. Only manganese ions are drawn for simplicity. Open (solid) circles denote Mn^{4+} (Mn^{3+}) ions. The occupied e_g orbital is shown for each Mn^{3+} ion. Arrows show the arrangement of Mn spin moments as deduced for the $R=$ Tb compound.

ferent spin-ordering pattern from that of the *A*-site-disordered compound. In this paper, we report on a different type of spin ordering in the *A*-site-ordered compound $\mathrm{TbBaMn_2O_6}$, which was revealed by neutron-diffraction technique. The antiferromagnetic phase transition is accompanied by the change in the stacking pattern of charge-ordered/orbital-ordered MnO_2 sheets along the *c* axis. The identical change in the charge/orbital ordering has been also found in diffraction studies on the Sm derivative $\mathrm{SmBaMn_2O_6}$.

Polycrystalline samples of $R=$ Sm and Tb were prepared by a solid-state reaction. After repeating the sintering process at 1600–1700 K in an Ar flow, the resulting ceramics were annealed at about 1000 K in an oxygen atmosphere. The details of the procedure are described elsewhere.[4] The almost perfect ordering of *R* and Ba was confirmed by the (001) reflection in the x-ray-diffraction and neutron-diffraction patterns. The *A*-site ordering is also manifested by the charge ordering transition at a high temperature.[4] Figure 1(a) shows a metal-insulator transition at $T_{\mathrm{CO}}\sim 470$ K and 380 K for the Tb and Sm compounds, respectively. A measurement of magnetization using a superconducting quantum interference device magnetometer reveals that phase-transition temperatures of antiferromagnetism, T_N, are about 200 K and 260 K for the Tb and Sm compounds, respectively, as shown by arrows in Fig. 1(b). The Curie-like behavior below T_N in the Tb compound is due to the paramagnetic large Tb moments, which have been found to align antiferromagnetically below 13 K.

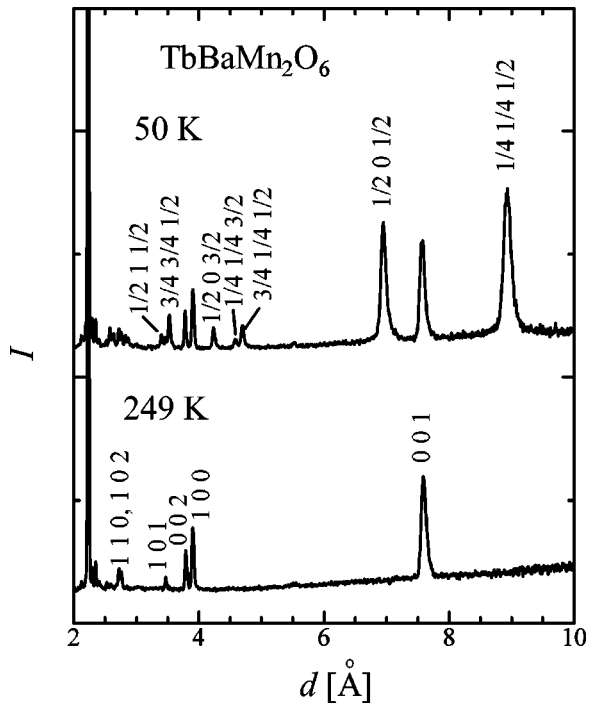

FIG. 3. Time-of-flight neutron-diffraction patterns of $\mathrm{TbBaMn_2O_6}$ at 50 K and 249 K, below and above the spin-ordering temperature ($T_N\sim 200$ K). The 50 K pattern is shifted upwards to avoid an overlap. The indices are based on the primitive tetragonal unit cell of $a_p\times a_p\times 2a_p$.

Powder neutron diffraction was measured using a time-of-flight (TOF) diffractometer Vega, KEK, Japan. The temperature was controlled in an accuracy of within 0.2 K by a closed-cycle 4-K refrigerator. The obtained patterns of $\mathrm{TbBaMn_2O_6}$ at 50 K and 249 K are displayed in Fig. 3. Here we note that at 249 K the 001 peak is clearly observed, which manifests the Tb/Ba ordering. Comparing the two TOF patterns, some additional peaks are found at 50 K (below T_N). Because Tb moments show the least ordered component at the temperature, the peaks can be ascribed to antiferromagnetic ordering of Mn spin moments. In fact, the magnetic peaks are observed to be much larger in the neutron pattern at 4 K due to an ordering of large Tb moments.

All the magnetic peaks can be indexed by two modulation wave vectors, (1/4 1/4 1/2) and (1/2 0 1/2), in the pseudo-tetragonal setting with $a_p\times a_p\times 2a_p$ (see the inset of Fig. 1) as shown in the 50-K data in Fig. 3 (a). Here a_p denotes the cell parameter of the cubic perovskite. The modulation vectors are translated into (1/4 1/4 1/4) and (1/2 0 1/4) in the primitive cubic setting. This evidently shows that the magnetic unit cell consists of four Mn-O sheets, which is twice as long as the *c* axis of the magnetic unit cell of the so-called CE-type magnetic structure. The CE-type antiferromagnetism is characterized by the propagation vectors of the magnetic peaks of (1/4 1/4 1/2) and (1/2 0 1/2) in the cubic setting, and quite often observed in the *A*-site-disordered perovskite manganites such as $\mathrm{La_{1/2}Ca_{1/2}MnO_3}$,[7] $\mathrm{Pr_{1/2}Ca_{1/2}MnO_3}$,[9] and $\mathrm{Nd_{1/2}Sr_{1/2}MnO_3}$,[8] in which the charge-ordered/orbital-ordered MnO_2 sheets stack along the *c* axis without any phase shift, and each spin moment antiferromag-

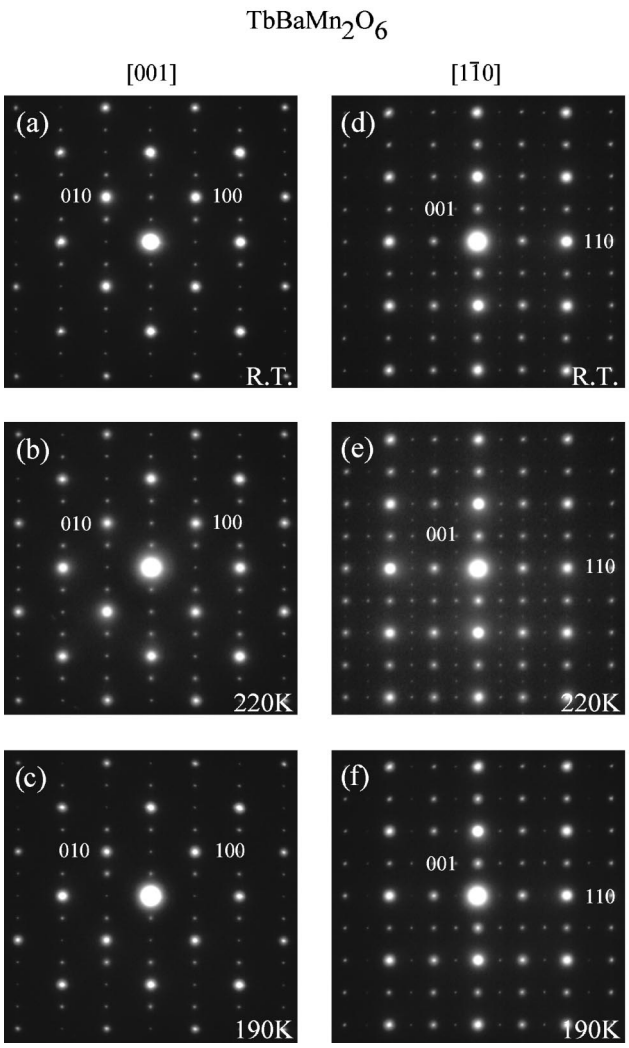

FIG. 4. Electron-diffraction patterns of $TbBaMn_2O_6$: (a)–(c) [001]-zone-axis patterns at room temperature (290 K), just above T_N (220 K), and just below T_N (190 K). (d)–(f) [1 $\bar{1}$ 0]-zone-axis patterns at room temperature (290 K), just above T_N (220 K), and just below T_N (190 K). The indices are based on the primitive tetragonal unit cell of $a_p \times a_p \times 2a_p$.

netically aligns along the *c* axis. The longer period of the magnetic unit cell of $TbBaMn_2O_6$ along the *c* axis as observed indicates that charge-ordered/orbital-ordered Mn-O sheets stack in a different way from the hitherto known one.[5]

To investigate the stacking of the MnO_2 sheets in $TbBaMn_2O_6$, we performed transmission electron microscopy (TEM) studies above and below T_N. Thin samples for electron-diffraction studies were prepared by crushing the material into fine fragments with CCl_4, which were then dispersed on Cu grids coated with holy-carbon support films. Electron-diffraction studies were carried out as a function of temperature with a Hitachi HF-3000S TEM operating at 300 kV. In Figs. 4(a)–4(c) the [0 0 1]-zone-axis electron-diffraction patterns of $TbBaMn_2O_6$ at 290 K, 220 K, and 190 K are shown, respectively. At all the temperatures, a series of superlattice reflections with a modulation wave vector of (1/4 1/4 0) are clearly observed. The superlattice reflections should originate from the charge and orbital ordering, as in the case of other manganese oxides with the Mn average valence of ~ 3.5, which is also consistent with the metal-insulator behaviors shown in Fig. 1(a).[6] The [1 $\bar{1}$ 0]-zone-axis electron-diffraction patterns are shown in Figs. 4(d)–4(f). At room temperature and 220 K, another series of superlattice reflections with a modulation wave vector of (1/2 1/2 1/2) are clearly observed. These superlattice reflections are ascribed to the four-sheet period of stacking of MnO_2 sheets with charge ordering of checkerboard type, as shown in Fig. 2(a).[6] Hereafter we call the stacking manner the "*AABB* type." The superlattice reflections are found to disappear at around T_N. Figures 4(e) and 4(f) show the results just above and below T_N (220 and 190 K), respectively. The same kind of change in the stacking pattern at the antiferromagnetic transition has been confirmed also for $SmBaMn_2O_6$ by TEM as well as by the synchrotron x-ray-diffraction study (at the beamline 1*A*, Photon Factory, KEK) on a single crystal.

The disappearance of the (1/2 1/2 1/2) series of reflections in electron-diffraction and x-ray-diffraction can be attributed to the change in the stacking pattern of the charge/orbital-ordered MnO_2 sheets. The *c*-axis length of the *crystallographic* unit cell reduces to $2a_p$, which is the same as the primitive unit cell shown in the inset of Fig. 1. Therefore, there are three possible stacking patterns with the period of one or two Mn-O sheets, as shown in Figs. 2(b)–2(d). In each MnO_2 sheet, Mn^{3+} (filled circles) and Mn^{4+} (open circles) ions align alternately. Mn^{3+} ions form orbital stripes along the [1 $\bar{1}$ 0] direction. The most plausible one is the *ABAB*-type stacking shown in Fig. 2(b). Here the charge-ordered/orbital-ordered Mn-O sheets stack along the *c* axis with a phase shift of $\pm \mathbf{a}$, alternately. It is noteworthy that the charge ordering is of the NaCl type, where the Madelung-type Coulomb energy gain is maximal. In the figure, the alignment of spin moments deduced by the neutron study is also shown by arrows. (Note that the direction of the spin moments is not determined yet.) The spin moments align antiferromagnetically between the second-nearest Mn-O sheets. Next candidate is the *AAAA*-type stacking [Fig. 2(c)], which is usually observed in the case of the *A*-site *disordered* manganese oxide system such as $Pr_{1/2}Ca_{1/2}MnO_3$, $La_{1/2}Ca_{1/2}MnO_3$, and $Nd_{1/2}Sr_{1/2}MnO_3$. However, the spin alignment in these compounds is of the CE type as aforementioned. If one tries to reproduce the observed magnetic peak positions in the *AAAA*-type stacking model, one has to assume that the alignment of spin moments along the *c* axis is of $\uparrow\uparrow\downarrow\downarrow$ type. It is unrealistic that every Mn^{4+}-Mn^{4+} pair in two neighboring MnO_2 sheets would couple ferromagnetically. Another stacking pattern with the period of $2a_p$ is shown in Fig. 2(d), where $3y^2-r^2$ and $3x^2-r^2$ orbitals are alternately occupied in Mn^{3+} chains. This is also unlikely the case, because the (1/4 1/4 0) series of reflections would be extinct in this stacking model. In addition, Mn^{4+} (Mn^{3+}) ions would form simple antiferromagnetic (ferromagnetic) chains along the *c* axis with this type of charge and orbital ordering.

From the above arguments, it is concluded that the *A*-site-ordered perovskite manganite $R\mathrm{BaMn_2O_6}$ shows different types of spin/charge/orbital ordering both above and below T_N from the conventional case of the *A*-site-disordered perovskite manganese oxide compounds. The *A*-site-ordering has two effects on the physical properties of a perovskite system. One is the disappearance of randomness in the Coulomb potential. This promotes ordering of the charge degree of freedom, giving rise to the charge ordering at a higher temperature as observed. The other is the existence of two inequivalent apical oxygen ions in every $\mathrm{MnO_6}$ octahedron. Namely, there are two kinds of Mn—O—Mn bonds along the *c* axis in the *A*-site-ordered perovskite. This may stabilize the *AABB*-type stacking as observed in the temperature range between T_{CO} and T_N. For example, a shorter Mn—O—Mn bond may favor a $\mathrm{Mn^{3+}}$ and $\mathrm{Mn^{4+}}$ pair because the Coulomb interaction would be larger. Longer bonds may connect two charge-ordered/orbital-ordered $\mathrm{MnO_2}$ planes with no shift, because a $\mathrm{Mn^{3+}O_6}$ octahedron elongated along the *a* or *b* axis tend to stack on another octahedron with the elongation along the same direction in order to minimize the lattice strain energy.

Next, let us discuss the possible origins of the switching of a stacking manner at T_N. The relative shift of a_p along the *a* axis with a stacking of two charge-ordered/orbital-ordered $\mathrm{MnO_2}$ sheets modifies the contribution from each of the various interaction. On one hand, the shift gains the Coulomb energy between the two charge-ordered $\mathrm{MnO_2}$ sheets, because the two manganese ions with different valences are neighboring along the *c* axis. For the same reason, the shift also increases the electron transfer between the two Mn ions along the *c* direction. On the other hand, the superexchange interaction between the t_{2g}^3 electron spins always favors antiferromagnetic coupling between the two neighboring manganese ions in adjacent $\mathrm{MnO_2}$ sheets. Only when two adjacent $\mathrm{MnO_2}$ sheets in charge/orbital ordering are stacked without any shift, all the spin pairs along the *c* axis can be aligned antiferromagnetically, because of the zigzag-type spin structure with the charge/orbital stripes in a $\mathrm{MnO_2}$ sheet. The observed change from the *AABB* type in the paramagnetic phase to the *ABAB* type in the antiferromagnetic phase is apparently contradictory to this simple anticipation taking account of the superexchange interaction between the t_{2g}^3 electron spins alone. It is thus not so straightforward to understand why the magnetic ordering triggers the *ABAB*-type stacking below T_N. The clue to this problem might be obtained by the future study on the structural change in the course of the magnetic transition.

In summary, we have revealed that the magnetic structure in the *A-site-ordered* manganese oxide perovskite $\mathrm{TbBaMn_2O_6}$ is different from the so-called CE type, which is widely seen in the *A-site-disordered* compounds. Powder neutron diffraction as well as electron diffraction and x-ray diffraction has proved that the antiferromagnetic phase transition is accompanied by a change in a stacking pattern of charge-ordered/orbital-ordered $\mathrm{MnO_2}$ sheets, from the *AABB* type to the *ABAB* type.

We thank I. Solovyev for fruitful discussions, and R. Kumai, H. Sawa, Y. Wakabayashi, H. Nakao, M. Toda, and R. Tazaki for their support in the synchrotron x-ray measurements.

[1] See for example, Y. Tokura and N. Nagaosa, Science **288**, 462 (2000); Y. Tokura, *Colossal Magnetoresistance Oxides* (Gordon and Breach, Amsterdam, 2000).

[2] F. Millange, V. Caignaert, B. Domenges, and B. Raveau, Chem. Mater. **10**, 1974 (1998).

[3] T. Nakajima, H. Kageyama, and Y. Ueda, J. Phys. Chem. **63**, 913 (2002).

[4] D. Akahoshi, M. Uchida, Y. Tomioka, T. Arima, Y. Matsui, and Y. Tokura (unpublished).

[5] J.B. Goodenough, Phys. Rev. **100**, 564 (1955).

[6] M. Uchida, D. Akahoshi, R. Kumai, Y. Tomioka, T. Arima, Y. Tokura, and Y. Matsui, J. Phys. Soc. Jpn. (to be published).

[7] E.O. Wollan and W.C. Koehler, Phys. Rev. **100**, 545 (1955).

[8] H. Kawano, R. Kajimoto, H. Yoshizawa, Y. Tomioka, H. Kuwahara, and Y. Tokura, Phys. Rev. Lett. **78**, 4253 (1997).

[9] Z. Jirak, S. Krupicka, Z. Simsa, M. Dlouha, and S. Vratislav, J. Magn. Magn. Mater. **53**, 153 (1985).